Proceedings of the 20th International Conference on Soil Mechanics and Geotechnical Engineering– Rahman and Jaksa (Eds)

Simulation of mechanical dispersion by an anisotropic pore-network model

Simulation of Mechanical dispersion by anisotrope Pore Network Model

Xinghao Zhang & Dantong Lin, Liming Hu
State Key Laboratory of Hydro-Science and Engineering, Department of Hydraulic Engineering, Tsinghua University, China, xinghao-20@mails.tsinghua.edu.cn

ABSTRACT: Mechanical dispersion occurs when solute transports in porous media. Equivalent pore-network model (EPNM) has been successfully used in describing the pore structure and the seepage process in pore scale, and has potential to simulate mechanical dispersion of solute transport. In this study, an EPNM is established to study the influence of pore structure on mechanical dispersion. The validity of the model is verified by comparing with experimental data. Outflow curves obtained by the EPNMs with various pore structures are investigated to study the relationship among parameters for mechanical dispersion and pore structures. Results show that dispersivity is positively related to throat curvature and negatively related to coordination number and anisotropic degree.

RÉSUMÉ : La dispersion mécanique se produit lorsque le soluté se déplace dans un milieu poreux.Le modèle de réseau interstitiel équivalent (epnm) a été utilisé avec succès pour décrire la structure interstitielle et le processus d'infiltration, ce qui pourrait être utile pour simuler la dispersion mécanique du transport des solutés.Dans cette étude, nous avons établi un epnm pour étudier l'effet de la structure des pores sur la dispersion mécanique.La validité du modèle est vérifiée par comparaison avec les données expérimentales.On a étudié les courbes d'écoulement des epnms avec différentes structures poreuses et la relation entre les paramètres de dispersion mécanique et la structure poreuse.Les résultats montrent que la dispersion est positivement corrélée avec la courbure laryngée et négativement corrélée avec le nombre de coordonnées et le degré d'anisotropie.

KEYWORDS: Mechanical dispersion; anisotropy; porous media; pore-network model; dispersivity.

1 INTRODUCTION

With the development of economy and industrial progress, the pollution caused by human production activities has been paid more and more attention. The infiltration of contaminated surface water into subsurface aquifers will result in the contamination of groundwater. Consequently, it is of great significance to study the transport mechanism of pollutants in groundwater for predicting the movement of pollutants and for controlling and remedying groundwater pollution. In porous media, the movement mechanism of pollutants with groundwater mainly includes convection and dispersion (Bear, 2018). Dispersion consists of effective molecular diffusion and mechanical dispersion. molecular diffusion is causing by the Brownian motion of the solute. Due to the complex pore structure of porous media, the micro-velocity and direction distribution of groundwater in it are not uniform, causing the solute to disperse. This phenomenon is called mechanical dispersion. There are many studies on mechanical dispersion at macroscopic scale, which considers the porous medium as a continuum and the dispersion in groundwater as the combined effect of effective diffusion of solute due to concentration gradient and mechanical dispersion due to groundwater flow in pore structure of soils. The convection-dispersion equation is proposed, and the one-dimensional form is as follows:

$$\frac{\partial C}{\partial t} + v\frac{\partial C}{\partial x} = D\frac{\partial^2 C}{\partial x^2} \quad (1)$$

where C is solute concentration, v is the pore velocity, and D is dispersion coefficient. The mechanical dispersion is determined by the pore structure so that its mechanism and influence factors can only be described at the microscopic level. Taloy (1953) explained the mechanism of mechanical dispersion in a cube. As shown in Fig. 1, in a cube, the solute in the center is going fast, while the solute close to the wall is going slow, causing longitudinal mechanical dispersion. The complex pore structure can also cause mechanical dispersion. As shown in Fig. 2. The flow direction and velocity are different in different seepage channels. The solute separates and mixes with water flow, causing longitudinal and horizontal mechanical dispersion. Due to the complexity of pore structure, an appropriate method is needed to study mechanical dispersion in it. The pore network model is a good choice.

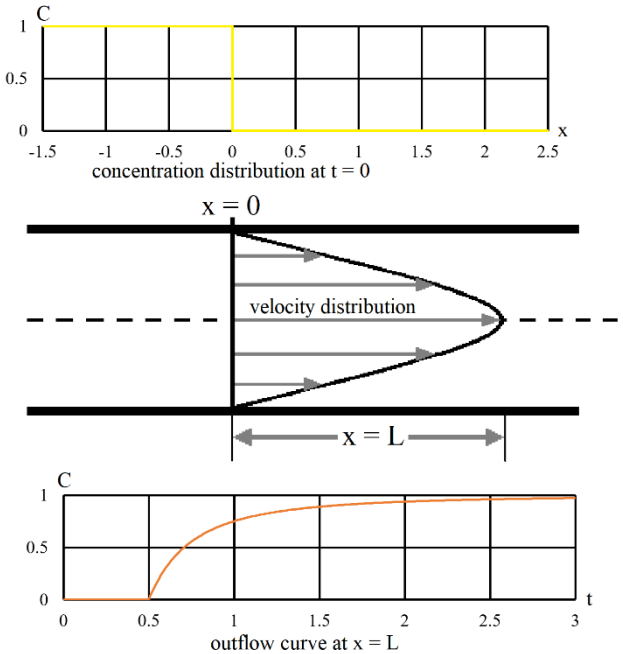

Figure 1. Longitudinal mechanical dispersion in a cube

The pore network model simplifies the pore structure to a network of connected pore bodies and throats. Traditional pore network model is extracted from the pore structure. But, Scanning, reconstruction and extraction of pore structure is time-consuming so it is hard to research the influence of the pore structure on mechanical dispersion.

The equivalent pore-network model (EPNM) is a kind of model which is established only based on physical statistical parameters. EPNM is widely used in the study of seepage and

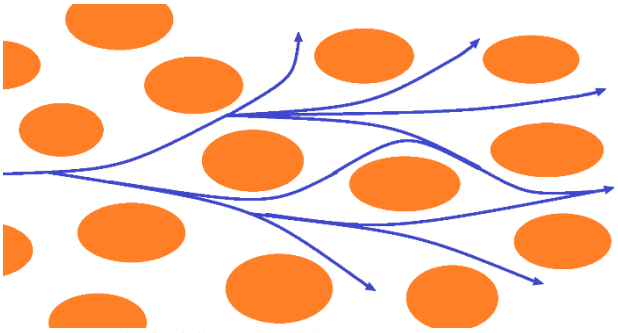

Figure 2. Mechanical dispersion in the pore structure

solute transport. Fatt (1956) established a two-dimensional equivalent pore network model composed of cube tubes. Nicholson et al. (1971) proposed the three-dimensional equivalent pore network model and used it to calculate the two-phase flow. Raoof (2009) proposed a 26-coordination number EPNM and simulated the adsorption process in porous media. Gao (2012) compared the equivalent pore network model with the pore reconstruction model, and found that the results were highly consistent. Therefore, the equivalent pore network model was considered to be effective in studying seepage flow. Zhang et al. (2015) established Knudsen diffusion in a cylindrical tube and applied it to the equivalent pore network model to study the influencing factors of apparent permeability in gas seepage. Zhang et al. (2021) proposed an anisotropy EPNM to reflected the anisotropy of porous media. Lin et al. (2021) simulated the surface deposition process of colloidal particles and analyzed the pore-scale parameters including the distribution of pore-throat adhesion efficiency in EPNM.

The above work shows that EPNM can be used for seepage calculation and solute transport research. However, the study on mechanical dispersion by EPNM has not been reported yet. Mechanical dispersion is an important process of solute transport in porous media, which is strongly influenced by pore structure (Bear, 2018). In this study, we perform the following steps to obtain the relationship between the pore structure and the mechanical dispersion coefficient. First, determine the geometric parameters and use them to construct the EPNM. Second, give hypothesis, parameters of the liquid and boundary conditions and calculate the steady-state flow field in EPNM. Third, give hypothesis, initial conditions and boundary conditions and calculate the solute transport process. Finally, mechanical dispersion coefficient is obtained by fitting the outflow flow curve which is obtained by statistics.

2 METHOD

2.1 *Geometry and flow field*

In the EPNM, the calculation domain is a cuboid. As shown in Fig. 3, Pore bodies are spheres and aligned on the point of the grid. Pore bodies are connected by throats which are cylinders. Grid element length is the length of the side of the cube grid, pore radius is generated from a given distribution, the coordination number refers to the average number of throats connected by a pore body and the pore-throat curvature determines the throat radius which can be calculated by BACON equation (Acharya et al., 2004):

$$T_i = \frac{r_i \sin(\pi/8)}{[l - r_i \sin(\pi/8)]^n} \tag{1a}$$

$$r_{ij} = lT_iT_j(T_i^{1/n} + T_j^{1/n})^{-n} \tag{1b}$$

where l is gird element length, r_{ij} is the radius of throat ij, r_i is the radius of pore body i, T_i is the parameters of pore body i and n is throat curvature. Throat number ratio means the ratio of the number of throats in X and Y directions. In the simulation, the number of throats in the Z direction is the same as the number of throats in the Y direction.

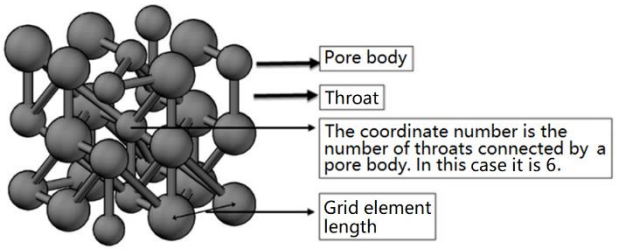

Figure 3. A structure diagram of EPNM

In the model, the radius of pore body is generated randomly according to a given distribution. A single pore body can connect 26 throats at most. The throats are randomly generated according to the coordination number and the proportion in X, Y and Z directions.

In order to get the steady-state flow field, the left and right boundaries are set as constant pressure boundaries, the other boundaries are set as no flux boundaries. Each pore body has only one pressure value at a time and the flow in each throat is considered laminar so that the flux of every throat can be calculated by (Raoof et al., 2012):

$$Q_{ij} = \frac{\pi r_{ij}^4}{8\mu l_{ij}}(p_i - p_j) \tag{1}$$

where r_{ij} and l_{ij} is the radius and length of the throat, respectively, p_i and p_j are pressure value at both ends of the throat, and μ is the kinetic viscosity of the fluid. Because the fluid is considered incompressible, the sum of the flux Q_{ij} from the upstream throats is the same as that of downstream throats, which can be written as:

$$\sum_j Q_{ij} = 0 \tag{2}$$

The flux Qj, for each pore body, can be calculated as:

$$Q_j = \sum_j^{N_{up}} Q_{ij} \tag{3}$$

where N_{up} is the number of throats from which the liquid flows into this pore body.

2.2 *Solute transport*

The left boundary is set as a constant concentration boundary, the right boundary is set as an open boundary, the other boundaries are set as no flux boundaries. Before calculation, the solute concentration in the computed field is set to 0.

Assume that the solute only moves with the flow and that there's only one concentration in one pore body or one throat at a time, so that solute mass exchange occurs only at the interface of pore body and throat. The change of concentration in pore body j can be written as:

$$V_j \frac{dC_j}{dt} = \sum_j^{N_{up}} Q_{ij}C_{ij} - Q_jC_j \tag{4}$$

where V_i and C_i are the volume and the liquid concentration in this pore body, respectively. The change of concentration in throat ij can be written as:

$$V_{ij}\frac{dC_{ij}}{dt} = Q_{ij}C_i - Q_{ij}C_{ij} \quad (5)$$

where V_{ij} and C_{ij} are the volume and the liquid concentration in this throat. C_i is the liquid concentration in the pore body which is upstream of this throat.

The outflow curves of solute by EPNM with different pore structure parameters were calculated by space averaging.

2.3 *Model validation*

To study the validation of the model, a column experiment is carried out. The diameter of the column is 3 cm and the height of it is 15 cm. Small glass beads with a diameter of 570 μm were filled in the column. The porosity was between 0.30 and 0.32 by controlling the amount of glass beads filling. Before the experiment, the pore was filled with deionized water. During the experiment, 150 mg/L methyl orange solution with a total of 0.8 times of pore volumes was injected from the top of the column at a flow rate of 4.1 m/d, and sufficient deionized water is continuously injected. The concentration of the outflow is collected and measured on the opposite side. By fitting the outflow curve, the hydrodynamic dispersion coefficient is 6.58×10^{-7} m^2/s, and the molecular diffusion coefficient of solute in liquid is 10^{-10}~10^{-9} m^2/s at room temperature, which is relatively small, so the influence of molecular diffusion can be ignored (Bear,2018).

To simulate this case in EPNM. PFC3D is used to stack 1000 balls with a radius of 570 μm, and the pore structure was obtained by controlling the friction coefficient to make the porosity between 0.30 and 0.32, as shown in Fig. 4. The distribution of pore body radius, defined as the local inradius, is as shown in Fig. 5. The average coordination number is 8. When the pore-throat curvature is 0.12, the average pore-throat radius in the EPNM is consistent with extracted average pore radius which is 39.8 μm.

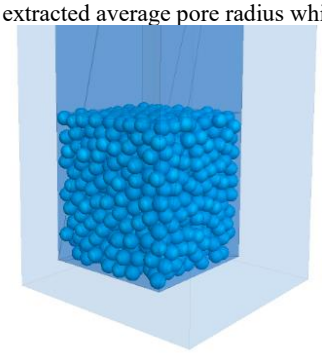

Figure 4. A packing model of balls

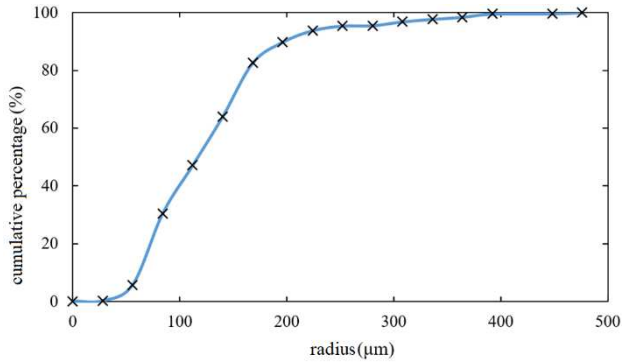

Figure 5. Pore body radius accumulation curve

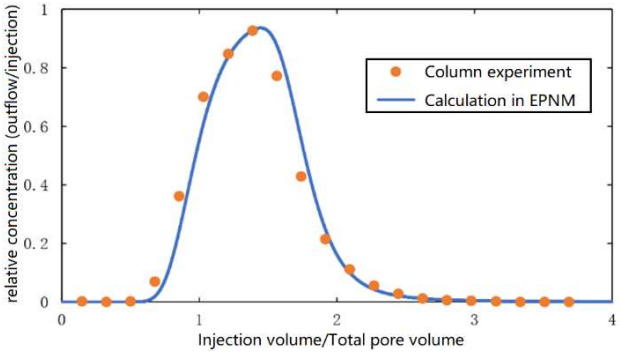

Figure 6. Pore body radius accumulation curve

The information extracted from the pore structure and the flow rate is used to construct the model. In order to ensure that the length of the model was the same as the 15 cm in the column experiment, the model size was set as 379×10×10. After the injection of standard solution with 0.8 times the pore volume, sufficient clean water was continuously injected, and the outflow curve was calculated and compared with the outflow curve in the column experiment, as shown in Fig. 6. The two curves are in good agreement, so that the model is effective.

2.4 *Simulation scenarios*

In the simulation, pore bodies are aligned on the points of a 20×10×10 grid as shown in Fig. 7. Pore body radius distribution is the normal distribution the standard deviation is 10% of the mean value. Dynamic viscosity is 0.001 Pa·s. A sufficient standard solution (C_0=1) is injected from the left of the model. The whole simulation ends when the outflow concentration is greater than 0.99. The mechanical dispersion coefficient is obtained by fitting the outflow curve. Although the model is three-dimensional, it simulates one-dimensional situations, so only longitudinal dispersion is discussed. The simulation scenarios are shown in Table 1.

Table 1. Simulation scenarios

NO	1	2	3	4
Average pore body radius(μm)	1-10	10	10	10
Grid element length(μm)	3.9-39	39	39	39
Throat curvature	1	0.2-2	1	1
Coordinate number	8	8	2-26	8
Throat number ratio	1	1	1	0.2-5

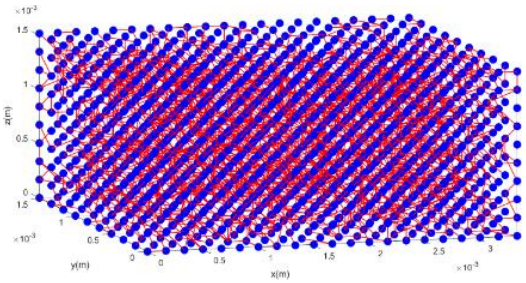

Figure 7. The geometry of the EPNM

After the geometry is determined, The mechanical dispersion

coefficient D is proportional to the pore velocity v, which can be written as:

$$D = \alpha|v| \tag{6}$$

where α is the overall amplification.

3 RESULTS AND DISCUSSION

3.1 *Influence of the scaling*

Equally scaling of the model can be achieved by adjusting the pore body radius and element length in equal proportion. The variation of dispersivity with scaling is shown in Fig. 8. The dispersivity is determined by the geometry of the pore structure. After scaling, the process of mechanical dispersion does not change under the assumptions in this study. It's just that the units of length have changed. The dispersivity is proportional to the scale because the unit of dispersivity is the same as the unit of length. Slight fluctuations are due to the randomness of the model generation process.

3.2 *Influence of throat curvature*

Since throat radius is inversely related to throat curvature, throat radius can be changed by adjusting throat curvature. The influence of throat curvature on the dispersivity is shown in Fig. 9. When the throat curvature increases, the throat radius decreases and the volume of throats relative to the pore bodies decreases. As a result, the solute stays relatively short in the throats and mixes more quickly in the pore bodies. Correspondingly, the dispersivity increases.

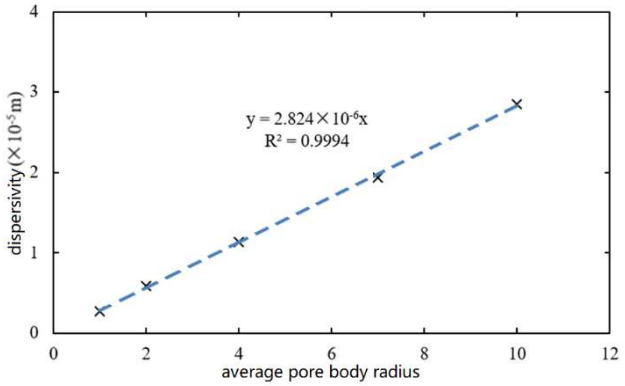

Figure 8. The effect of scaling on dispersivity

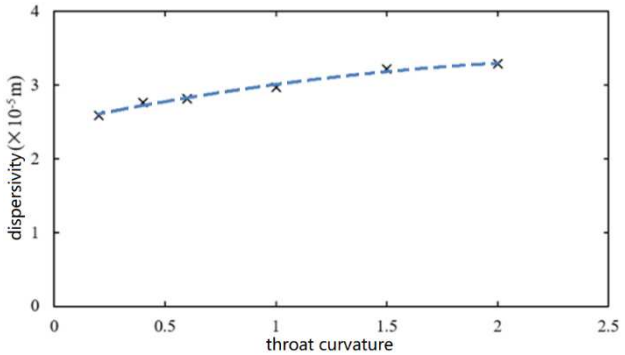

Figure 9. The effect of throat curvature on dispersivity

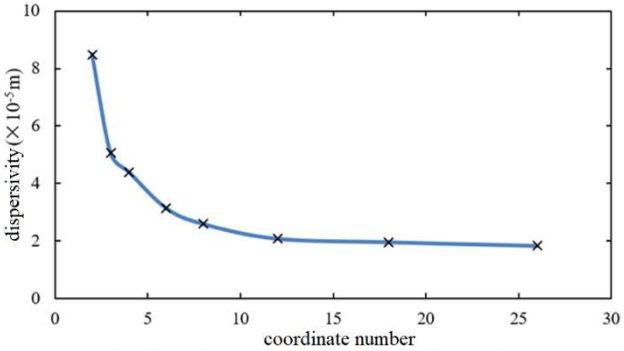

Figure 10. The effect of coordination number on dispersivity

3.3 *Influence of coordinate number*

The coordination number refers to the number of pore-throats connections by each pore body. The coordination number can reflect the connectivity of the pore structure. The higher the average coordination number is, the better the connectivity is and the higher the permeability is.

The influence of coordination number on dispersivity is shown in Fig. 10. The dispersivity decreases with the increase of the coordination number. Coordination number affects the degree of connectivity between the pore bodies. When coordination number is low, throats are few so that complete transport accesses are more difficult to form, then the solute will be difficult to find a relatively straight access to the downstream and the difference of different accesses is large. Consequently, the dispersivity is larger compared to the situation with the high coordination number.

3.4 *Influence of throat number ratio*

The influence of throat number ratio β on dispersivity is shown in Fig. 11. When the throat number ratio is 1, the model is isotropic and the dispersivity is maximum. In other cases, the model is anisotropic and we can define anisotropic degree α as follows:

$$\alpha = \beta + \frac{1}{\beta} \tag{7}$$

Different throat number ratio affects the transport path. As the throat number ratio increases or decreases from 1, the anisotropy degree increases and the access is more concentrated in one direction so that the flow direction of each seepage access tends to be the same. Consequently, it is harder for the solute to disperse into another access. For the above reasons, the dispersivity is maximum in the case of isotropy (the ratio of throat number ratio is 1) and decreases when the throat number ratio increases or decreases from 1.

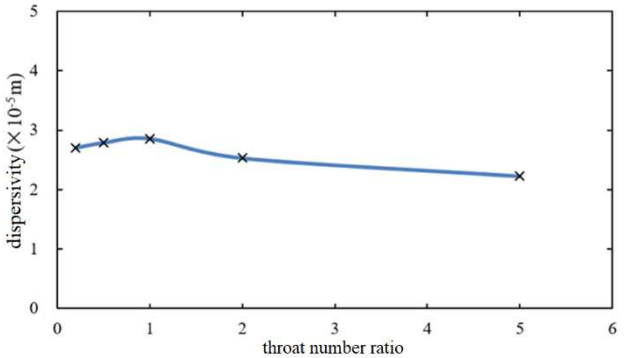

Figure 11. The effect of throat number ratio on dispersivity

5 CONCLUSIONS

The influence of pore structure on solute transport is investigate by means of pore-network model. The main findings are as follows:

(1) As the throat curvature increases, the throat radius decreases, causing the longitudinal dispersivity increases.

(2) As the coordination number decreases, the connectivity of the pore structure becomes better, causing the longitudinal dispersivity increases.

(3) Longitudinal Dispersivity is maximum when the pore-throat number ratio is 1. As the pore-throat number ratio increases or decreases from 1, The anisotropy degree of the model increases, causing the longitudinal dispersivity decreases.

6 ACKNOWLEDGEMENTS

The National Key Research and Development Program of China (2020YFC1806502), National Natural Science Foundation of China (51979144), and the State Key Laboratory of Hydro-Science and Engineering (2020-KY-01) funded this research.

7 REFERENCES

Acharya R C, van der Zee S E A T M, and Leijnse A, 2004. Porosity-permeability properties generated with a new 2-parameter 3D hydraulic pore-network model for consolidated and unconsolidated porous media[J]. *Advances in Water Resources*, 27 (7): 707-723.

Fatt I, 1956. The network model of porous media[J]. *Transactions of the AIME*, 207 (1).

Taylor G, 1953. Dispersion of soluble matter flowing slowly through a tube.pdf[J]. Proceedings of the Royal Society of London. Series A, *Mathematical and Physical Sciences*, 219 (1137): 186-203.

Bear J, 1996. Modeling Transport Phenomena in Porous Media[J]. Springer New York.

Lin D, Hu L, Bradford S A, Zhang X, and Lo I M C, 2021. Simulation of colloid transport and retention using a pore-network model with roughness and chemical heterogeneity on pore surfaces[J]. *Water Resources Research*, 57 (2).

Nicholson D, and Petropoulos J H, 1971. Capillary Models for Porous Media: III. Two-phase flow in a three-dimensional network with Gaussian radius distribution[J]. *Journal of Physics D Applied Physics*, 4 (2): 181.

Zhang P, Hu L, Wen Q, and Meegoda J N, 2015. A multi-flow regimes model for simulating gas transport in shale matrix[J]. *Géotechnique Letters*, 5 (3): 231-235.

Raoof A, Nick H M, Wolterbeek T K T, and Spiers C J, 2012. Pore-scale modeling of reactive transport in wellbore cement under CO2 storage conditions[J]. *International Journal of Greenhouse Gas Control*, 11: S67-S77.

Gao S Y, Meegoda J N, and Hu L M, 2012. Two methods for pore network of porous media[J]. *International Journal for Numerical and Analytical Methods in Geomechanics*, 36 (18): 1954-1970.

Zhang D, Zhang X, Guo H, Lin D, Meegoda J N, and Hu L, 2021. An anisotropic pore-network model to estimate the shale gas permeability[J]. *Scientific Reports*, 11 (1): 7902.